Adaptive CAD-Model Building Algorithm for General Planar Microwave Structures

Jan De Geest, Tom Dhaene, Niels Faché, *Member, IEEE,* and Daniël De Zutter, *Senior Member, IEEE*

***Abstract*—A new adaptive technique is presented for building multidimensional parameterized analytical models for general planar microwave structures with a predefined accuracy and based on full-wave electromagnetic (EM) simulations. The models can be incorporated in a circuit simulator and the time required to calculate the circuit representation of a practical network is reduced by several orders of magnitude compared to full EM simulations. Furthermore, the accuracy of the results is significantly better compared to the circuit models used in state-of-the-art computer-aided design tools.**

***Index Terms*— Approximation methods, circuit simulation, computer-aided engineering, design automation, modeling.**

I. Introduction

PRECISE characterization of high-frequency interconnects is very important for circuit simulation and optimization purposes. Different numerical electromagnetic (EM) analysis techniques (e.g., method of moments,[1] finite elements,[2] finite-difference time domain, etc.) can be used to characterize the interconnects. Those techniques, although very accurate, are often not practical to use directly for circuit design and optimization, due to the large amount of computer time required. Circuit simulators, on the other hand, are very fast. However, models for high-frequency interconnects used in circuit simulators are often inaccurate or even unavailable. Building accurate models based on EM simulations for use in circuit simulators makes it possible to combine the speed of circuit simulators and the accuracy of EM simulators in fast and precise computer-aided design (CAD) software.

Planar structures are fully characterized by their scattering matrix. The scattering parameters are a function of frequency and of certain geometrical parameters. The geometrical parameters can be related to the dimensions of the metallizations in the circuit (such as the widths, lengths, etc. of the strips), but also substrate parameters (such as the substrate thickness, dielectric constant, losses, etc.) can be considered. The parameter ranges, i.e., the minimum and maximum value of each of the geometrical parameters and frequency, define the parameter space.

The technique described here—in what follows, referred to as multidimensional adaptive parameter sampling (MAPS)—builds a global fitting model for the relevant scattering parameters of an interconnection structure with a predefined accuracy. The algorithm consists of two adaptive loops: an adaptive modeling loop (see Section III) and an adaptive sampling loop (see Section IV). Geometrical dependencies and frequency dependencies (see Section V) are handled separately. Examples are given to illustrate the technique (see Section VI). The work presented in this paper has been submitted for patenting in the U.S. by the Hewlett-Packard Company, Santa Rosa, CA.

Manuscript received January 1999; revised June 1999.

J. De Geest and D. De Zutter are with the Department of Information Technology (INTEC), University of Gent, B-9000 Gent, Belgium (e-mail: jdgeest@intec.rug.ac.be).

T. Dhaene and N. Faché are with HP-EEsof, B-9000 Gent, Belgium.

Publisher Item Identifier S 0018-9480(99)07173-2.

[1] HP Momentum, Hewlett-Packard Company, Santa Rosa, CA.

[2] HP HFSS, Hewlett-Packard Company, Santa Rosa, CA.

II. Prior Solutions

Numerous efforts have been spent to build models for general interconnection structures based on full-wave EM simulations. Commonly used techniques include look-up tables, curve-fitting techniques, and neural networks. A common drawback is the lack of knowledge about the accuracy of the resulting models. The accuracy of a model is usually tested after the model has been generated. If the accuracy is insufficient, a new model is built. This is repeated until the model reaches the desired accuracy.

In the look-up table approach, a number of data points are calculated up front on a fixed grid and stored in a database. During the extraction, some interpolation techniques, often simple linear or quadratic interpolation, are used. Interpolation of points in a look-up table is a highly localized operation, where only data points in the neighborhood of the value required are used. Furthermore, the disk space required for multidimensional table-based models can be excessively high.

Interpolation techniques can also be used to fit some kind of model on the data before it is stored in a database [1]–[4]. An approach based on look-up tables offers some flexibility to the designer, although the accuracy of these techniques is often questionable. In some parts of the parameter space, too many data points might be available (oversampling), while in other parts, there might be too few data points (undersampling). Oversampling means a waste of time, while undersampling means a poor model quality. Curve-fitting techniques often have some artifacts such as excessive humps, overshoots, and unwanted oscillations.

Another fairly new modeling technique uses artificial neural networks (ANN's) to generate parameterized models [5]–[9]. A number of training and testing samples is chosen in the geometrical parameter space and along the frequency axis, and an ANN is trained to model the circuit behavior. ANN's can handle highly nonlinear behavior and high-dimensional models. Furthermore, the size of the models does not grow

exponentially with the dimension. However, it is hard to find a good topology (number of hidden layers and nodes), and training can take a long time and is hard to survey. Hence, it is difficult to ensure the quality of ANN models.

Our new MAPS technique aims at building compact parameterized models for general interconnection structures with a guaranteed accuracy. The model generation process is fully automatic and does not require any *a priori* knowledge about the circuit under study. Data points are selected efficiently to avoid oversampling and undersampling. The model complexity is automatically adapted. The algorithm converges when the desired accuracy is reached. The model covers the whole parameter and frequency space and can easily be used for optimization purposes.

III. Building the Models in an Adaptive Way

When it comes to building models of general linear time-invariant interconnection structures, the scattering matrix representation has some interesting characteristics and advantages over alternative approaches. The scattering matrix $\overline{S}$ of a linear time-invariant reciprocal circuit is a symmetrical $N_p \times N_p$ matrix ($S_{ij} = S_{ji}$), with N_p the number of external ports to the circuit. For linear time-invariant passive circuits, the scattering parameters are bounded, i.e., $|S_{ij}| \leq 1$. Furthermore,

$$\overline{Q} = \overline{E} - \overline{S}^{+}\overline{S} \tag{1}$$

is a positive semidefinite matrix (with $\overline{E}$ the $N_p \times N_p$ unit matrix and $\overline{S}^{+}$ the Hermitian conjugate of $\overline{S}$). This implies that

$$Q_{ii} = 1 - \sum_{j=1}^{N_p} |S_{ij}|^2 \geq 0 \tag{2}$$

(with $i = 1, \cdots, N_p$). The real and the imaginary part of S_{ij} are modeled separately.

The scattering parameters S (in what follows the indexes i and j are omitted, unless they are necessary to differentiate between the scattering parameters) are represented by multidimensional polynomials (*multinomials*)

$$\begin{aligned} S(f, X) \approx & M(f, X) \\ &= \sum_m \beta_m(f) B_m(X) \\ &= \sum_m \beta_m(f) \prod_{i=1}^{n} x_i^{e_{mi}}. \end{aligned} \tag{3}$$

The same set of basis functions $B_m(X)$ is used over the whole frequency range of interest. The basis functions only depend on the coordinates $X = [x_1, \cdots, x_n]$ (with n the number of geometrical parameters) in the parameter space R, while the weights β_m only depend on the frequency f. The weights can be calculated by fitting the set of data points X_s ($s = 1, \cdots, N_s$) on (3)

$$S(f, X_s) = \sum_m \beta_m(f) B_m(X_s). \tag{4}$$

The data points X_s ($s = 1, \cdots, N_s$) consist of an initial data point distribution plus a number of additional data points selected by the adaptive data point selection algorithm (see Section IV). Instead of solving the system of equations (4) directly, for numerical stability and efficiency reasons, the basis functions $B_m(X)$ are used as the starting point to build a set of orthonormal multinomials $P_k(X)$. To this end, the following algorithm is used:

$$P_0(X) = \frac{B_0(X)}{\sqrt{\sum_{s=1}^{N_s} B_0(X_s)^2}} \tag{5}$$

for $k = 0$ and

$$P_k^{(g)}(X) = B_k(X) - \sum_{l=0}^{k-1} \alpha_l P_l(X) \tag{6}$$

$$P_k(X) = \frac{P_k^{(g)}(X)}{\sqrt{\sum_{s=1}^{N_s} P_k^{(g)}(X_s)^2}} \tag{7}$$

for $k \geq 1$. From the condition

$$\sum_{s=1}^{N_s} P_k(X_s) P_l(X_s) = \delta_{kl} = \begin{cases} 1, & k = l \\ 0, & k \neq l \end{cases} \tag{8}$$

the α_l can be calculated as follows:

$$\alpha_l = \sum_{s=1}^{N_s} P_l(X_s) B_k(X_s). \tag{9}$$

Using these orthonormal multinomials, (3) can be rewritten as

$$S(f, X) \approx M(f, X) = \sum_m C_m(f) P_m(X) \tag{10}$$

with

$$C_m(f) = \sum_{s=1}^{N_s} S(f, X_s) P_m(X_s). \tag{11}$$

The number of basis functions in (4) is increased until the error $E = |M - S|$ is lower than a given threshold (which is a function of the desired accuracy of the model).

When there is just one geometrical parameter ($n = 1$), the multinomial reduces to a simple polynomial. The model is expanded by increasing the degree of the polynomial $B_k(X) = x_1^k$. The initial data point distribution consists of the left end, right end, and center of the parameter space (which, in this case, is an interval).

When there are two or more geometrical parameters, the model can be expanded by increasing the degree of either one of the parameters. However, the parameters that have the most influence on the scattering parameters must be assigned the most degrees of freedom in the final model. Therefore, instead of expanding the model evenly in each direction, the model must be extended the most in the direction of the parameter that has the biggest influence. Prior to building the multidimensional model, for each of the geometrical parameters x_i a one-dimensional model is built to get an idea about the influence each of the geometrical parameters has

on the modeled scattering parameters. In this model, x_i varies over its whole range, while the other parameters x_k (for $i \neq k$) are kept constant at their midpoint value. The number of basis functions used for building a one-dimensional model for x_i is denoted by N_{Mi}. In general, the multidimensional basis functions can be written as

$$B_k(X) = x_1^{e_{k1}} x_2^{e_{k2}} \cdots x_n^{e_{kn}}. \tag{12}$$

For each exponent e_{ki}, a corresponding normalized exponent E_{ki} is calculated as follows:

$$E_{ki} = \frac{e_{ki}}{N_{Mi}}. \tag{13}$$

These normalized exponents are increased equally as the model is extended so e_{ki} are increased proportionally with N_{Mi}. In this way, the most degrees of freedom are given to the geometrical parameters that have the most influence on the modeled scattering parameters. When selecting a new basis function, the following rules apply.

1) From all possible new basis functions, retain the ones for which $\max\{E_{k1}, E_{k2}, \cdots, E_{kn}\}$ is minimal.
2) From the remaining basis functions, retain those for which $E_{k1} + E_{k2} + \cdots + E_{kn}$ is minimal.
3) From the remaining basis functions, retain those for which $\max\{e_{k1}, e_{k2}, \cdots, e_{kn}\}$ is minimal.
4) From the remaining basis functions, retain those for which $e_{k1} + e_{k2} + \cdots + e_{kn}$ is minimal.
5) From the remaining basis functions, select one as the new basis function.

The initial multidimensional data point distribution is generated by taking a number of uniformly distributed points along each x_i-axis. Here as well, the influence each of the geometrical parameters has, must be taken into account. The geometrical parameters that have the largest influence are sampled the most densely.

IV. Selecting New Data Points in an Adaptive Way

New data points are selected in such a way that a predefined accuracy Δ for the models is guaranteed. The process of selecting data points and building models in an adaptive way is often called *(reflective) exploration* [10]. Reflective exploration is useful when the process for obtaining the data is very costly, which is the case for full-wave EM simulators. Reflective exploration requires *reflective functions*, which are used to select a new data point. These reflective functions adapt as the model refines. The reflective function used in the MAPS algorithm is the difference between the "best fit" M_H, which is the current model, and the "second best fit" M_L

$$M_H(f, X) = \sum_{m=0}^{N_M - 1} C_m(f) P_m(X) \tag{14}$$

$$M_L(f, X) = \sum_{m=0}^{N_M - 2} C_m(f) P_m(X). \tag{15}$$

The new data point is selected near the maximum of the reflective function (R denotes the parameter space and Φ denotes the frequency range)

$$\max_{X \in R,\, f \in \Phi} \left| M_H(f, X) - M_L(f, X) \right| = \max_{X \in R,\, f \in \Phi} \left| C_{N_M - 1}(f) P_{N_M - 1}(X) \right|. \tag{16}$$

The algorithm converges when

$$\max_{X \in R,\, f \in \Phi} \left| C_{N_M - 1}(f) P_{N_M - 1}(X) \right| \leq \Delta \tag{17}$$

where Δ is the desired accuracy of the model. Expression (16) can be rewritten as

$$\max_{X \in R,\, f \in \Phi} \left| M_H(f, X) - M_L(f, X) \right| = \max_{X \in R,\, f \in \Phi} \left| E_H(f, X) - E_L(f, X) \right| \leq \Delta \tag{18}$$

where $E(f, X) = S(f, X) - M(f, X)$. This inequality is graphically represented in Fig. 1. Both $E_L(f, X)$ and $E_H(f, X)$ are limited to a small banded region. If $E_H(f, X) E_L(f, X) \leq 0$, the modeling error is guaranteed to be less than Δ, and convergence is reached. If $E_H(f, X) E_L(f, X) > 0$, this condition is not sufficient to guarantee an error less than Δ, thus, additional criteria are needed.

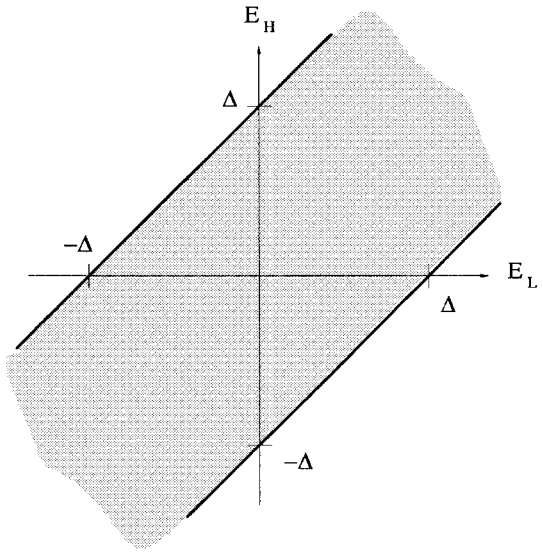

Fig. 1. E_H versus E_L.

The scattering parameters of a linear time-invariant passive circuit satisfy certain physical conditions (see Section III). If the model fails these conditions, it cannot accurately model the scattering parameters. The physical conditions act as additional reflective functions: if they are not satisfied, a new data point is chosen where the criteria are violated the most. Furthermore, if one of the scattering parameters has a local minimum or maximum in the parameter space, it is important to have a data point in the close vicinity to get an accurate approximation. Therefore, if there is no data point close to a local maximum or minimum of $M(f, X)$, the local extremum is selected as a new data point. For resonant structures, the power loss

$$Q_{ii} = 1 - \sum_{j=1}^{N_p} |S_{ij}|^2 \tag{19}$$

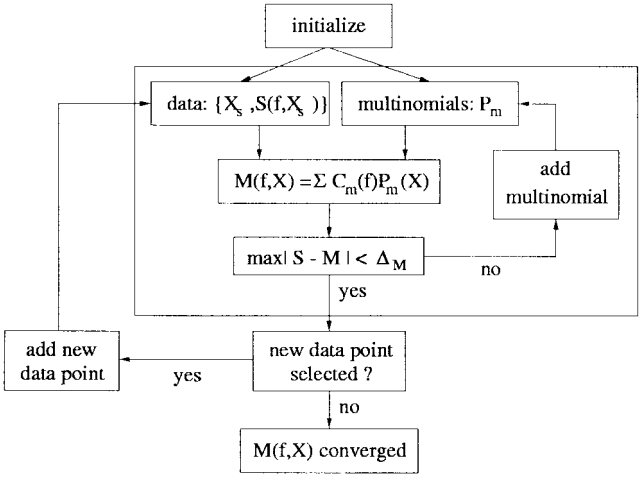

Fig. 2. Flowchart for the MAPS algorithm.

for a wave incident on the ith port has local maxima at the resonance frequencies. Again, to get an accurate approximation, a good knowledge of these local maxima is very important.

After each modeling loop, the error criteria are checked. If all of the criteria are satisfied, no new data point is selected and the MAPS algorithm converges. If a new data point is needed, it is calculated using HP Momentum. The model is adapted, and the adaptive data point selection loop is restarted. The complete flowchart of the algorithm is given in Fig. 2.

V. Adding Frequency Dependencies

In the previous two sections, it was explained how a model is built for the scattering parameters as a function of the geometrical parameters. However, the scattering parameters also depend on the frequency f (with $f \in \Phi$). The scattering parameters are generated using the commercially available full-wave EM simulator HP Momentum. The adaptive frequency sampling (AFS) algorithm [11] in HP Momentum selects a number of discrete frequencies $f_1, f_2, \cdots, f_{N_f}$ and builds a rational model for the scattering parameters over the desired frequency range Φ. The MAPS algorithm builds a multinomial model for each of the scattering parameters at each of the discrete frequencies f_j $(j = 1, \cdots, N_f)$. The number of basis functions used in each of these models, N_{Mj} for f_j, will, in general, be different at the different frequencies. In the end, the MAPS algorithm must result in a single model that covers the whole frequency range. The maximum number of basis functions used at any of the frequencies f_j is used as the number of basis functions in the global model $N_M = \max\{N_{M1}, N_{M2}, \cdots, N_{MN_f}\}$. Using the rational models built by AFS, the coefficients $C_m(f)$ (with $m = 0, \cdots, N_M - 1$) can then be calculated over the whole frequency range. Finally, polynomial or rational fitting techniques are used to compact the coefficients $C_m(f)$ before storing them in a database.

The whole MAPS modeling technique can be graphically represented in the following steps.

Step 1) The frequency response of the circuit is calculated at a number of data points in the parameter space using HP Momentum (Fig. 3). These discrete data points include the initial data points and the adaptively selected points. The AFS algorithm in HP Momentum selects a number of frequencies $f_1, f_2, \cdots, f_{N_f}$ and builds a rational model for the scattering parameters S over the desired frequency range Φ.

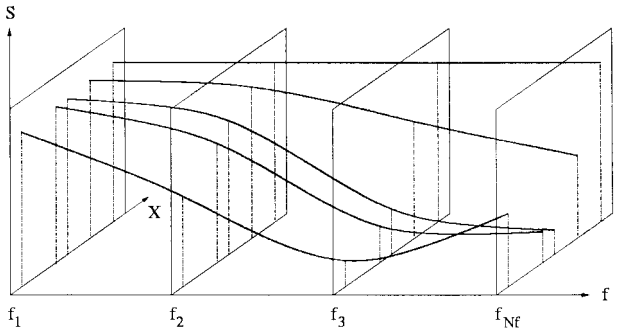

Fig. 3. Step 1: AFS rational models over the whole frequency range.

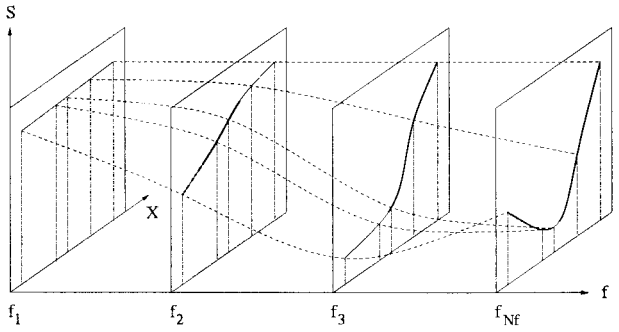

Fig. 4. Step 2: multinomial models at discrete frequencies.

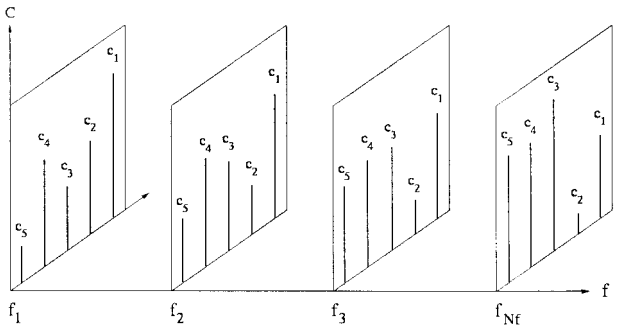

Fig. 5. Step 3: coefficients of orthonormal multinomials at discrete frequencies.

Step 2) At all frequencies $f_1, f_2, \cdots, f_{N_f}$, a multinomial model (as a function of the geometrical parameters) is fitted on the scattering parameters (Fig. 4).

Step 3) This model is written as a sum of orthonormal multinomials [see (10)]. The coefficients $C_m(f)$ of the multinomials are frequency dependent (Fig. 5).

Step 4) Using the AFS models built in Step 1, the coefficients C_m can be calculated over the whole frequency range (Fig. 6). These coefficients together with the orthonormal multinomials are stored in a database for use during extraction afterwards.

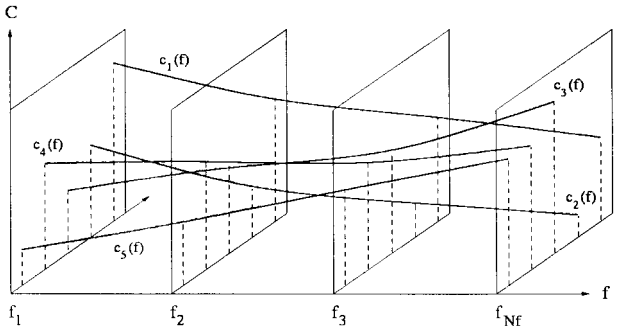

Fig. 6. Step 4: coefficients of orthonormal multinomials over the whole frequency range.

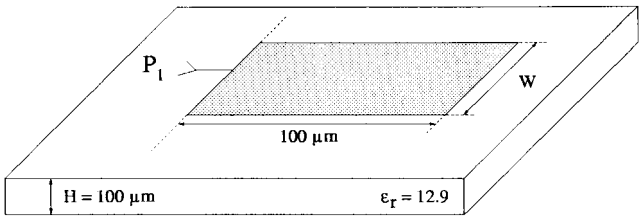

Fig. 7. Microstrip open end layout.

TABLE I
PARAMETER RANGES FOR THE MICROSTRIP OPEN END

	min	max
W	20 μm	120 μm
f	0 GHz	60 GHz

VI. EXAMPLES

In this section, a typical example is given to illustrate the technique described above and its application in circuit design. First, MAPS models are built for three basic junctions: an open end, a gap, and a tee junction. Afterwards, these basic models are used to accurately simulate a bandpass filter structure.

A. Microstrip Open End

Consider a microstrip open end on a 100-μm GaAs substrate with $\epsilon_r = 12.9$ (Fig. 7). The geometrical parameter included in the model is the width of the strip W. The ranges for W and the frequency f are given in Table I. The relevant scattering parameter is S_{11}. The desired accuracy of the model is $\Delta = -60$ dB. The initial data point distribution consists of three widths: $W = 20$, $W = 70$, and $W = 120$ μm. The value of S_{11} over the required frequency range is calculated using HP Momentum. There are four frequencies selected by the AFS feature of HP Momentum: 0, 20, 40, and 60 GHz. At these four frequencies, separate models are built for the real and imaginary part of S_{11}. The adaptive sample-selection algorithm selects three additional samples: $W = 40$, $W = 100$, and $W = 32$ μm.

The polynomial models for S_{11} (real and imaginary part) at each of the discrete frequencies, along with the selected data points, are shown in Figs. 8 and 9. The final models are shown in Figs. 10 and 11. For verification purposes, another 20 data points are simulated using HP Momentum, and the results are compared to the MAPS model. The maximum deviation is -62.4 dB ($= 0.0008$), which is better than the desired accuracy of -60 dB ($= 0.001$). Figs. 12 and 13 show a comparison between the results from HP Momentum, a commercially available circuit simulator, and the MAPS model for a specific width $W = 50$ μm (which was not used during model generation). As expected, the results from HP Momentum and the MAPS model correspond very well (they are virtually indistinguishable on the figure), while the results from the circuit simulator differ significantly from the full-wave results.

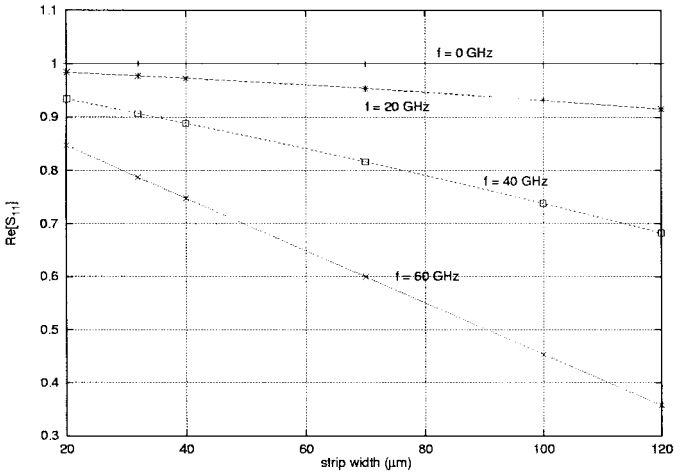

Fig. 8. Open end: polynomial models (and data points) for the real part of S_{11} at discrete frequencies.

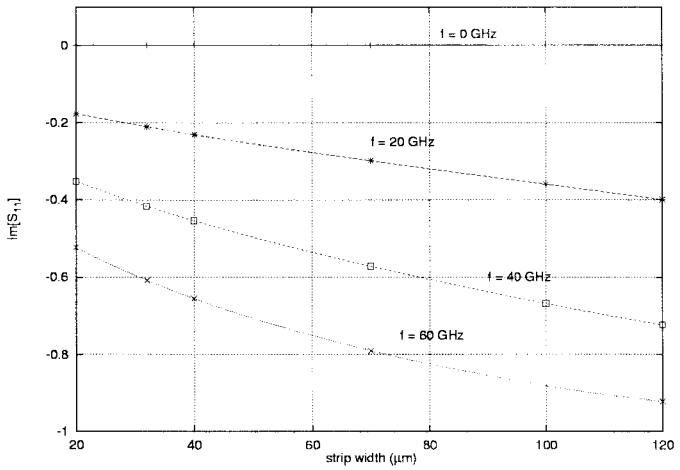

Fig. 9. Open end: polynomial models (and data points) for the imaginary part of S_{11} at discrete frequencies.

B. Microstrip Gap

The next example is a microstrip gap on a 100-μm GaAs substrate ($\epsilon_r = 12.9$). The layout is shown in Fig. 14. Here, there are two geometrical parameters: the width of the strip (W) and the width of the gap (G). The parameter ranges are given in Table II. The relevant scattering parameters are S_{11} and S_{12}. Again, the desired accuracy is set to $\Delta = -60$ dB. First, two one-dimensional models are built: a first one is for $G = 10.5$ μm with W varying from 40 to 100 μm, and a

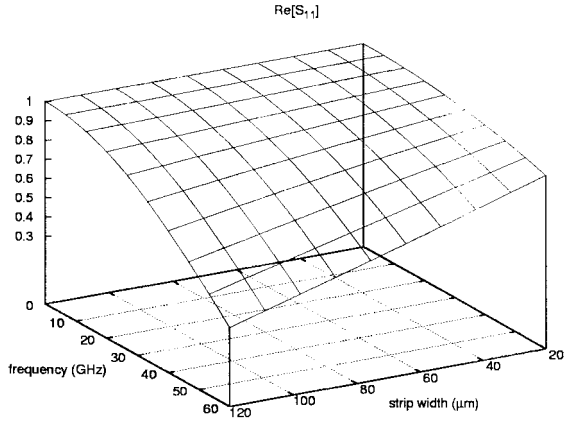

Fig. 10. Open end: MAPS model for the real part of S_{11} as a function of the frequency and the width of the strip.

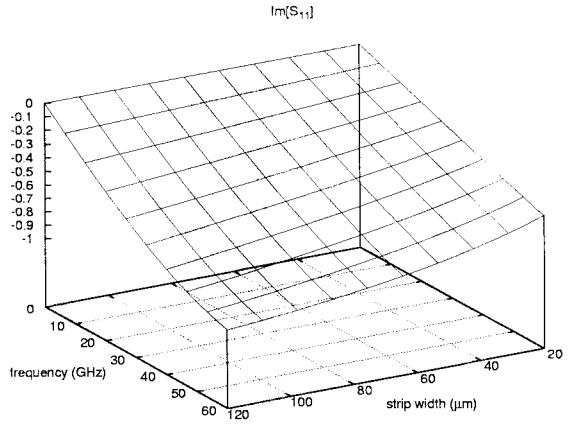

Fig. 11. Open end: MAPS model for the imaginary part of S_{11} as a function of the frequency and the width of the strip.

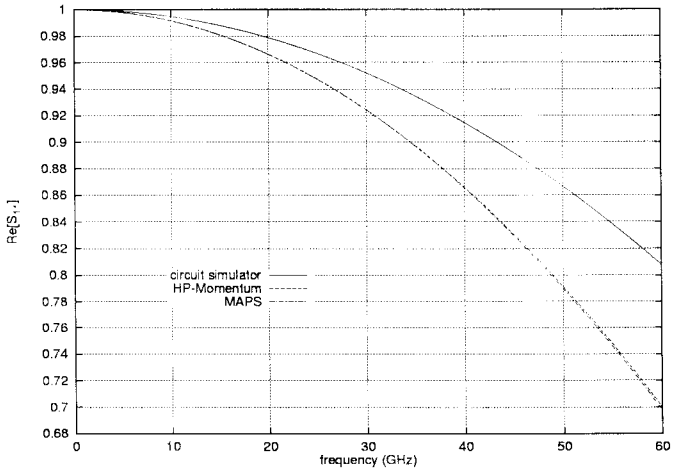

Fig. 12. Open end: comparison between the MAPS model, HP Momentum, and a circuit simulator of the real part of S_{11} for $W = 50$ μm.

second one for $W = 70$ μm and G varying from 1 to 20 μm. The first model requires five data points and the second model requires seven data points. The initial two-dimensional data point distribution consists of 21 points. An additional five data points are selected by the adaptive sampling algorithm (Fig. 15). Fig. 16 shows the imaginary part of S_{12} for $W = 64$ μm and $G = 2.9$ μm. Again, the results from the MAPS model correspond very well to the results from HP Momentum, while the results using a circuit simulator differ significantly. This is mainly caused by the fact that this specific gap structure is outside the validity range of the gap model in the circuit simulator.

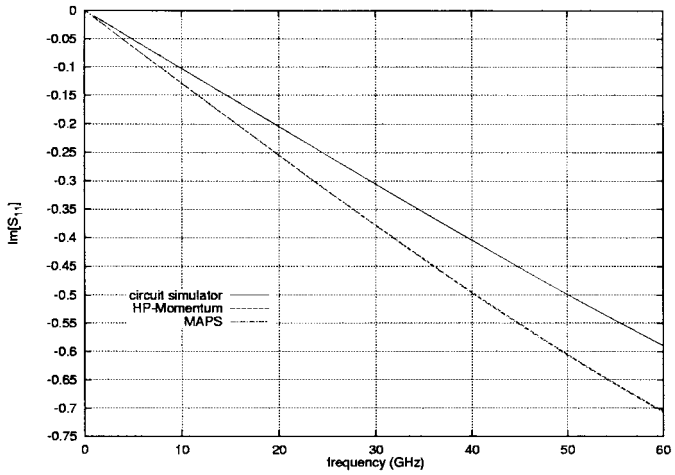

Fig. 13. Open end: comparison between the MAPS model, HP Momentum, and a circuit simulator of the imaginary part of S_{11} for $W = 50$ μm.

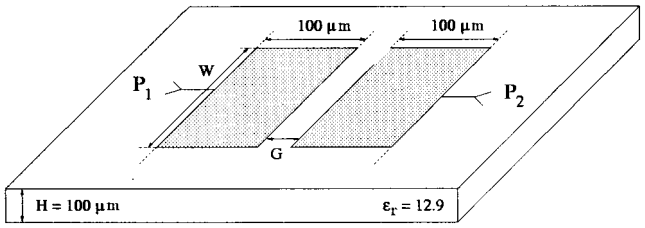

Fig. 14. Microstrip gap layout.

TABLE II
PARAMETER RANGES FOR GAP

	min	max
W	40 μm	100 μm
G	1 μm	20 μm
f	0 GHz	60 GHz

C. Microstrip Tee

Finally, consider a microstrip tee on a 100-μm GaAs substrate with $\epsilon_r = 12.9$ (Fig. 17). The geometrical parameters are the two widths W_1 and W_2. The ranges for W_1, W_2 and the frequency f are given in Table III. The relevant scattering parameters are S_{11}, S_{12}, and S_{13}. The desired accuracy of the model is $\Delta = -60$ dB. A total of 14 samples was needed during the model generation.

D. Bandpass Filter

The models built in the three previous examples are now used to simulate the bandpass filter structure given in Fig. 18. The structure is broken into nine elementary pieces (Fig. 19). The S-parameters of the elementary pieces are calculated using the MAPS models. Figs. 20 and 21 show S_{11}, and Figs. 22

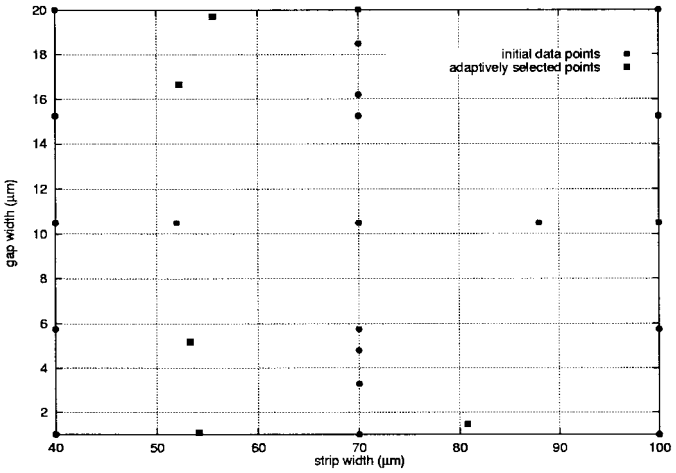

Fig. 15. Gap: data point distribution.

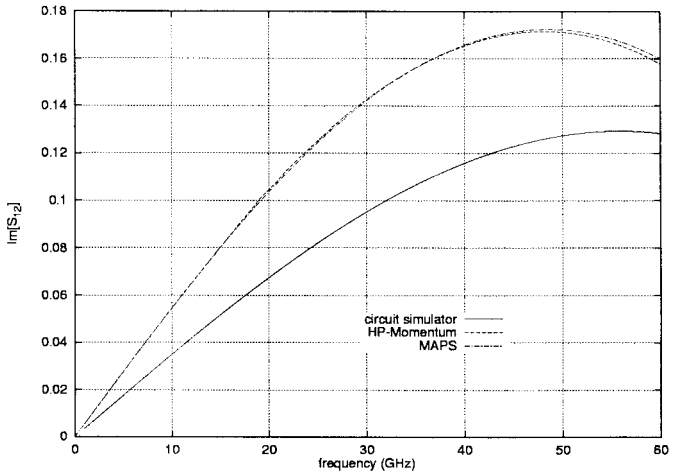

Fig. 16. Gap: comparison between the MAPS model, HP Momentum, and a circuit simulator of the imaginary part of S_{12} for $W = 64$ μm and $G = 2.9$ μm.

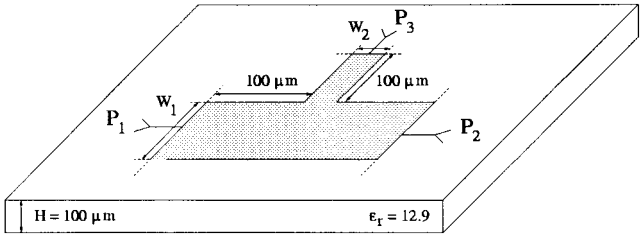

Fig. 17. Microstrip tee layout.

TABLE III
PARAMETER RANGES FOR TEE

	min	max
W_1	40 μm	120 μm
W_2	40 μm	120 μm
f	0 GHz	60 GHz

and 23 show S_{12} for the bandpass filter simulated with HP Momentum, with a circuit simulator and MAPS models. The results using the MAPS models are very close to the full-wave results, and yet the simulation only took a fraction of

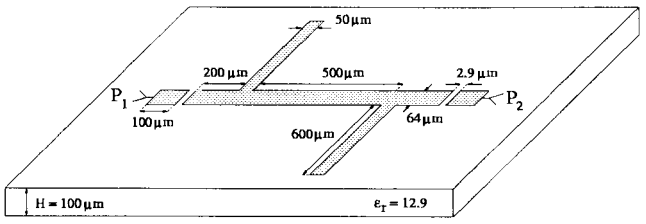

Fig. 18. Bandpass filter layout.

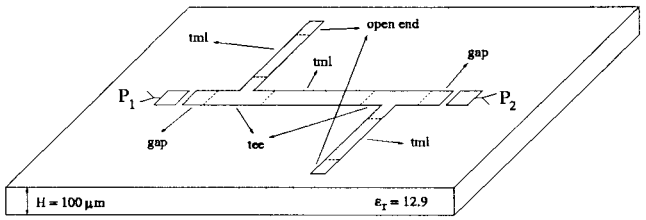

Fig. 19. Bandpass filter layout broken up into elementary junctions.

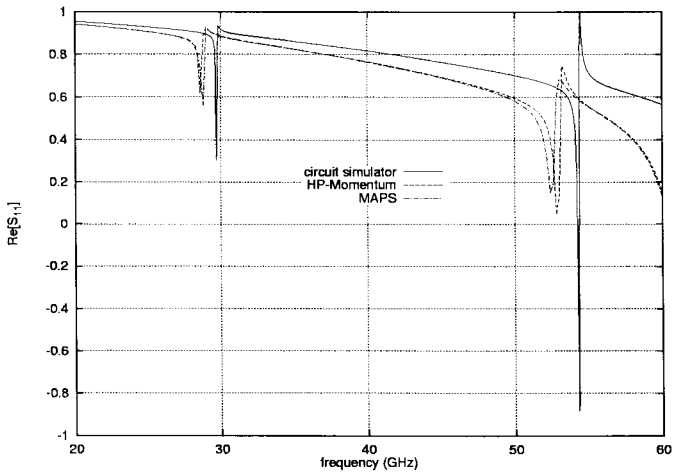

Fig. 20. Bandpass filter: real part of S_{11} simulated with the MAPS model, HP Momentum, and a circuit simulator.

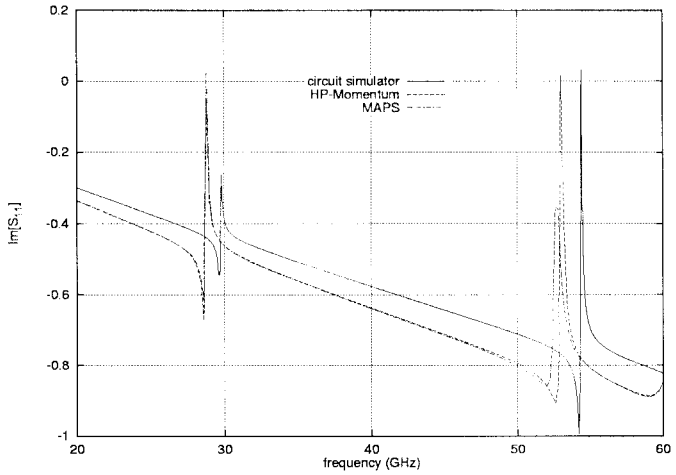

Fig. 21. Bandpass filter: imaginary part of S_{11} simulated with the MAPS model, HP Momentum, and a circuit simulator.

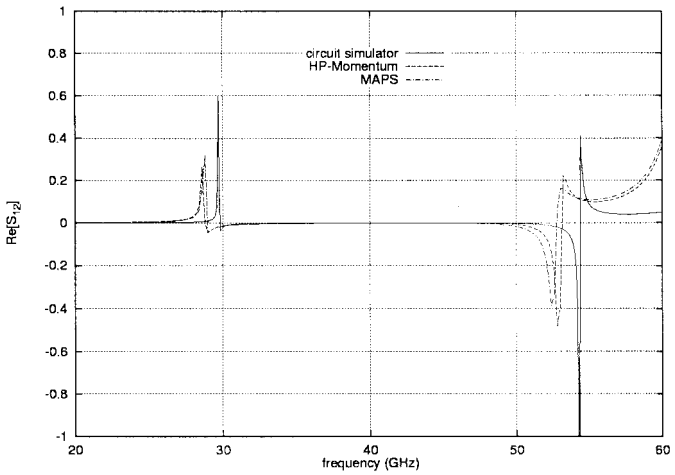

Fig. 22. Bandpass filter: real part of S_{12} simulated with the MAPS model, HP Momentum, and a circuit simulator.

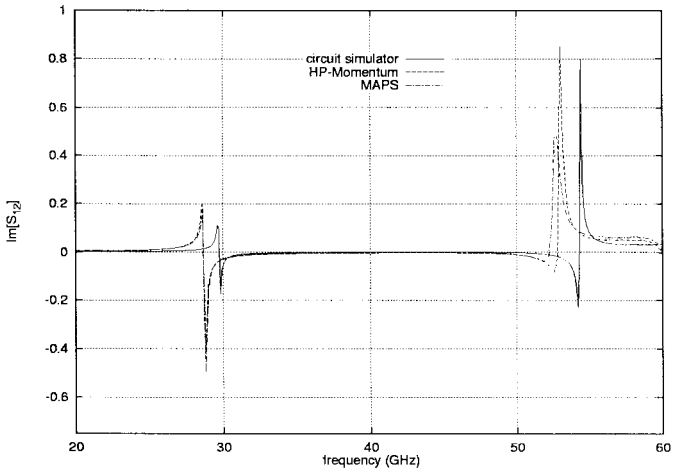

Fig. 23. Bandpass filter: imaginary part of S_{12} simulated with the MAPS model, HP Momentum, and a circuit simulator.

the time required for the full-wave simulation. Calculating 100 frequency points using the MAPS models took 2.11 s on an HP 720/50-MHz workstation, while calculating the 24 frequency points selected by AFS during the full-wave simulation required 1638 s. The MAPS models can predict the resonance frequencies very accurately, while the resonance frequencies found by the circuit simulator differ significantly from the full-wave results.

VII. Conclusion

A new technique—MAPS—was presented for building analytical models for general (multilayer) planar microwave structures. The models are based on full-wave EM simulations and have a guaranteed accuracy compared to full-wave results. They can be incorporated in a circuit simulator where they can replace existing state-of-the-art models, which are often inaccurate. Furthermore, the MAPS technique can be used to generate models for new geometries, for which models were previously unavailable.

To illustrate the technique, models were built for three microstrip components: an open end, a gap, and a tee. These models were then used to simulate a bandpass filter. The results using the MAPS models compare very well to a full-wave simulation of the whole filter structure, while the time required to obtain the results was only a fraction of the time required for the full-wave simulation. Using the MAPS models, the speed of a circuit simulator is combined with the accuracy of a full-wave EM simulator.

References

[1] J. W. Bandler, R. M. Biernacki, S. H. Chen, J. Song, S. Ye, and Q. J. Zhang, "Gradient quadratic approximation scheme for yield-driven design," in *Proc. IEEE MTT-S Symp. Dig.*, 1991, pp. 1197–1200.

[2] J. Carroll and K. Chang, "Statistical computer-aided design for microwave circuits," *IEEE Trans. Microwave Theory Tech.*, vol. 44, pp. 24–32, Jan. 1996.

[3] J.-F. Liang and K. A. Zaki, "CAD of microwave junctions by polynomial curve fitting," in *Proc. IEEE MTT-S Symp. Dig.*, 1993, pp. 451–454.

[4] D. E. Root, M. Pirola, S. Fan, W. J. Anklam, and A. Cognata, "Measurement-based large-signal diode modeling system for circuit and device design," *IEEE Trans. Microwave Theory Tech.*, vol. 41, pp. 2211–2217, Dec. 1993.

[5] G. L. Creech, B. J. Paul, C. D. Lesniak, T. J. Jenkins, and M. C. Calcatera, "Artificial neural networks for fast and accurate EM-CAD of microwave circuits," *IEEE Trans. Microwave Theory Tech.*, vol. 45, pp. 794–802, May 1997.

[6] T.-S. Horng and C.-C. Wang, "Microstrip circuit design using neural networks," in *Proc. IEEE MTT-S Symp. Dig.*, 1993, pp. 413–416.

[7] A. Veluswami, M. S. Nakhla, and Q.-J. Zang, "The application of neural networks to EM-based simulation and optimization of interconnects in high-speed VLSI circuits," *IEEE Trans. Microwave Theory Tech.*, vol. 45, pp. 712–723, May 1997.

[8] P. Watson and K. C. Gupta, "EM-ANN modeling and optimal chamfering of 90° CPW bends with air bridges," in *Proc. IEEE MTT-S Symp. Dig.*, 1997, pp. 1603–1606.

[9] A. H. Zaabab, Q.-J. Zhang, and M. Nakhla, "A neural network modeling approach to circuit optimization and statistical design," *IEEE Trans. Microwave Theory Tech.*, vol. 43, pp. 1349–1358, June 1995.

[10] U. Beyer and F. Smieja, "Data exploration with reflective adaptive models," *Computational Statistics Data Analysis*, vol. 22, pp. 193–211, 1996.

[11] T. Dhaene, J. Ureel, N. Faché, and D. De Zutter, "Adaptive frequency sampling algorithm for fast and accurate S-parameter modeling of general planar structures," in *Proc. IEEE MTT-S Symp. Dig.*, 1995, pp. 1427–1430.

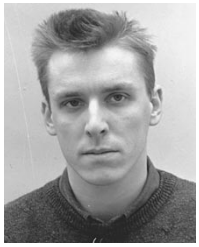

Jan De Geest was born in Gent, Belgium, on July 30, 1971. He received the electrical engineering degree and complementary studies degree in aerospace techniques from the University of Gent, Gent, Belgium, in 1994 and 1995, respectively, and is currently working toward the Ph.D. degree.

Since September 1995, he has been a Research Engineer in the Department of Information Technology, University of Gent. His main interests are in the modeling of planar microwave structures and high-frequency interconnects for use in CAD tools.

Tom Dhaene was born June 25, 1966, in Deinze, Belgium. He received the electrical engineering and Ph.D. degrees from the University of Gent, Gent, Belgium, in 1989 and 1993, respectively.

From September 1989 to December 1993, he was a Researcher in the Department of Information Technology (INTEC) University of Gent, where his research focused on different aspects of full-wave circuit modeling, transient simulation, and time-domain characterization of high-frequency and high-speed interconnections. Since 1993, he has been with the Electromagnetic Simulators Section, HP EEsof, Gent, Belgium His research interests are in the field of electromagnetic compatibility (EMC), reduced-order modeling, ANN's, adaptive modeling techniques, and system identification.

Niels Faché (S'92–M'92) received the electrical engineering and Ph.D. degrees from the University of Gent, Gent, Belgium, in 1986 and 1989, respectively.

In 1992, he cofounded Alphabit (acquired by HP EEsof in November 1994), the company that developed the first version of HP Momentum. He then became the HP Momentum R&D Project Manager for three years. In November 1997, he became a Product Marketing Manager at HP EEsof, where he is responsible for the marketing of microwave and EM products.

Daniël De Zutter (M'92–SM'96) was born in 1953. He received the M.Sc. degree in electrotechnical engineering, the Ph.D. degree, and a degree equivalent to the French Aggrégation or the German Habilitation from the University of Gent, Gent, Belgium, in 1976, 1981, and 1984, respectively.

From 1976 to 1984, he was a Research and Teaching Assistant at Gent University. From 1984 to 1996, he was with the National Fund for Scientific Research of Belgium. He is currently a Full Professor of electromagnetics in the Department of Information Technology (INTEC), University of Gent. Most of his earlier scientific work dealt with the electrodynamics of moving media. His research currently focuses on all aspects of circuit and EM modeling of high-speed and high-frequency interconnections, on EMC and EMI topics and on indoor propagation. He has authored or co-authored approximately 80 international journal papers and 95 papers in conference proceedings. He also co-authored *Electromagnetic and Circuit Modeling of Multiconductor Transmission Lines* (Oxford, U.K.: Oxford Univ. Press, 1993).

Dr. De Zutter is a member of the Electromagnetics Society. He received the 1990 Montefiore Prize presented by the University of Liège. He was a co–recipient of the 1995 IEEE Microwave Prize Award presented by the IEEE Microwave Theory and Techniques Society (MTT-S) for the best publication in the field of microwaves.